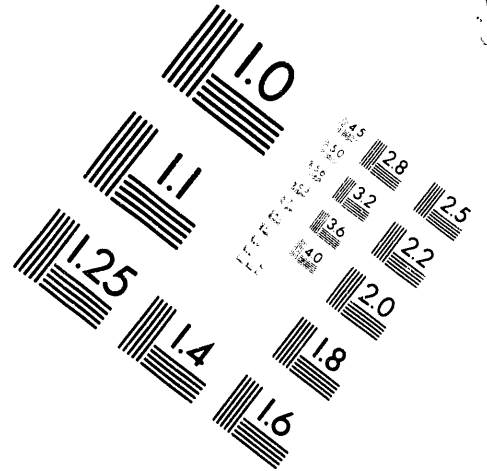
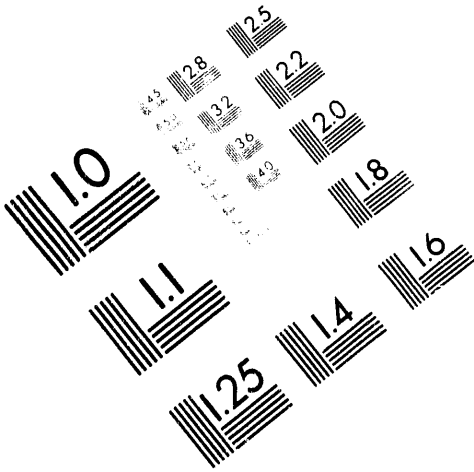




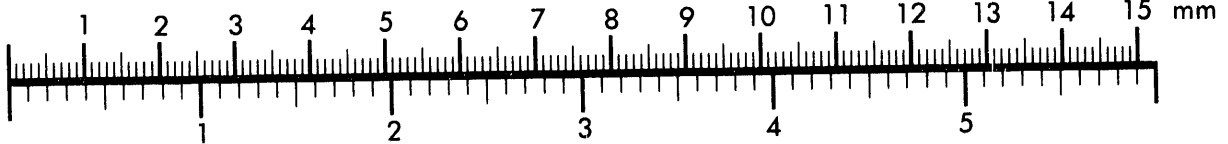
**AIM**

**Association for Information and Image Management**

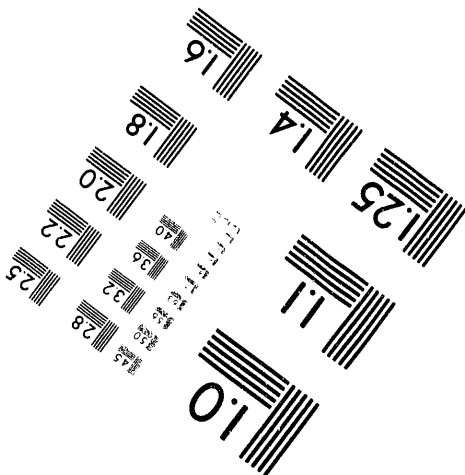
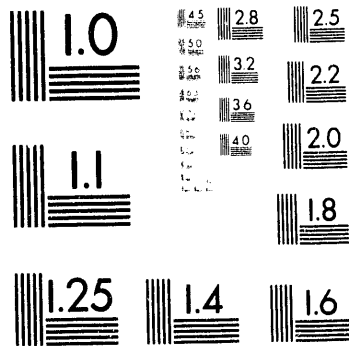
1100 Wayne Avenue, Suite 1100  
Silver Spring, Maryland 20910  
301/587-8202



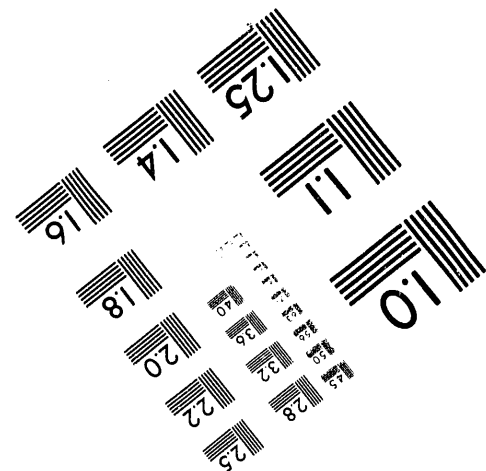
Centimeter



Inches



MANUFACTURED TO AIM STANDARDS  
BY APPLIED IMAGE, INC.



**1 of 1**

E66-M-93040  
CONF. 930121--3

## Numerical Investigations into the Formation of a 'High Temperature Reservoir'

Mike Shook  
Idaho National Engineering Laboratory  
PO Box 1625 MS 2107  
Idaho Falls, ID 83415

### Introduction

This paper summarizes an ongoing numerical modeling effort aimed at describing some of the thermodynamic conditions observed in vapor-dominated reservoirs, including the formation of a high temperature reservoir (HTR) beneath the "typical" reservoir. The modeled system begins as a hot water geothermal reservoir, and evolves through time into a vapor-dominated reservoir with a HTR at depth. This approach taken here to develop a vapor-dominated system is similar to that of Pruess (1985), and involves induced boiling through venting. The reservoir description is intentionally generic, but serves to describe a means of evolution of conditions observed (in particular) at The Geysers.

The formation of vapor-dominated geothermal reservoirs, such as The Geysers in northern California, Larderello in Tuscany, Italy, and Kamojang, Indonesia, has been subjected to intense scrutiny over the last several decades. These reservoirs are characterized in their native state by vapor-static pressure gradients and near-isothermal temperatures that extend vertically for up to thousands of meters. These conditions were explained conceptually by White et al. (1971) and Truesdell and White (1973) as manifestations of countercurrent flow of vapor (upward) and liquid (downward) in a "heat pipe" (Eastman, 1968). Steady state heat pipes result in large vertical heat flows with vanishingly small net mass flux.

It has been recognized since the early 1980's that, beneath portions of the "typical" vapor-dominated reservoir at The Geysers, there exists areas of high temperature; the temperature gradient in these zones approaches a conductive gradient. The transition between what has come to be known as the "typical" reservoir and the "high temperature reservoir" (HTR) occurs over a very small distance— on the order of hundreds of meters, and is not accompanied by any observed permeability barrier or other massive change in rock properties (eg, thermal conductivity) (Walters, et al., 1988). Evidence for the presence of a HTR at Larderello is less complete, and while most of the high temperature data can be explained by the presence of a liquid-dominated heat pipe at depth (Pruess et al., 1987), at least some of the temperature data is inconsistent with this model (Truesdell, 1991).

Several theories have been advanced concerning the formation of the HTR. Truesdell (1991) recently summarized three models for HTR formation, originally proposed by Drenick (1986). These three models can be summarized as: 1) an active liquid system, separated from the "typical" system by permeability barriers; 2) local heating from an intrusive, resulting in dry conditions and essentially

DISTRIBUTION OF THIS DOCUMENT IS UNLIMITED

MSH  
MASTER

conductive temperature gradients; and 3) a "fossil liquid system", which has recently (geologically speaking) boiled dry. Model 1 is discarded because such a permeability barrier has not been observed, and because of the observed pressure continuity between reservoirs. Truesdell discards model 3 from energy balance considerations and discrepancies in possible temperature gradients in the HTR, and ultimately offers a modification of Drenick's model 2, and suggests that the high temperature reservoir is due to recent downward extensions of an existing vapor-dominated reservoir into dry rock.

This study addresses the question of HTR formation numerically. The reservoir model and approach used is similar to that of Pruess (1985); however, vapor pressure lowering effects were included for the rock matrix. Results of this study indicate that a high temperature reservoir may occur as a steady state component of a "typical" vapor-dominated reservoir. Fractures within the HTR are dry; however, saturated conditions exist in the rock matrix. Pressures at depth follow a vapor pressure with depth relationship. Temperatures at depth are large (relative to saturated conditions) because of superheat in the fractures and vapor pressure lowering in the matrix. Drying out the fracture network at depth appears to be what drives the system to form a high temperature reservoir; however, adsorption in the rock matrix allows for saturated conditions to prevail.

### Numerical Model

The model used in this study is a one-dimensional, fractured, vertical reservoir. The Warren and Root (1963) dual porosity model is used, with matrix-matrix interactions allowed in the vertical direction. The dimensions of the reservoir are 100 m by 100 m areally, and 1200 m vertically. Fracture spacing is also 100 m. The permeability field used was  $10^{-14}$  m<sup>2</sup> (10 md) for the fracture network, and  $10^{-17}$  m<sup>2</sup> (10 md) for the rock matrix. Thermal properties of the rock were taken from the geothermal literature, and are summarized in Table 1. These properties were selected to be representative of Geysers rock properties.

Additional properties required in the simulation study include relative permeability and capillary pressures for the fractures and rock matrix. There are no published laboratory data for Geysers rock, and therefore these properties were selected somewhat arbitrarily. For relative permeabilities, the following functional form is used:

$$k_{rl} = k_{rl}^0 (S)^{e_l}, \quad k_{rv} = k_{rv}^0 (1 - S)^{e_v}$$

$$S = \frac{S_l - S_{lr}}{1 - S_{lr} - S_{vr}}$$

Parameters used for relative permeability are given in Table 1, and the relative permeability curves are shown in Figures 1 and 2. In the lower quarter of the reservoir, "matrix" relative permeabilities were used in the fractures and matrix alike. Rocks in the HTR are more thermally altered, and it was thought that changes in wettability (and therefore in relative permeability and capillary pressure) could be partially responsible for formation of the HTR.

Capillary pressures are of the form:

$$P_c = P_{c\text{-max}} (1 - S_l)^n$$

A maximum capillary pressure was arbitrarily selected as 1380 kPa (13.8 bars). We further assume that the full range of capillary pressure is also encountered in the fractures, albeit over a much smaller range of saturation values. This is done by assigning substantially more curvature to the capillary pressure curve in the fractures than in the matrix, and allows for capillary equilibrium between the two domains (Pruess et al., 1985). Capillary pressure curves are given in Figure 3.

The simulation model used in this study was TETRAD (Vinsome, 1991; Vinsome and Shook, 1993). A numerical grid of 24 vertical elements was selected, with vertical grid dimensions of 50 m. The fluid was assumed to be pure water in this preliminary study. Further studies are planned to include the effects of brine and noncondensable gases.

A final important feature of the reservoir model involves vapor pressure lowering (VPL). VPL effects were incorporated in the rock matrix by including adsorption, and was implemented in TETRAD in a manner described by Holt and Pingle (1992). Langmuir parameters A and B were as reported by Nghiem and Ramey (1991). The resulting vapor pressure ratio  $\beta$  vs. saturation is given in Figure 4.

### **Model Implementation**

Initial conditions for the base case simulation were hydrostatic equilibrium, and a constant (240°C) temperature. Pressure at the top of the reservoir was set at 3580 kPa, slightly above saturation pressure. A heat flux of 0.5 W/m<sup>2</sup> was proscribed at the base of the reservoir, and the top surface was held at constant temperature and pressure. All other boundaries were considered no-flow. In response to the heat flux at the bottom, the reservoir undergoes transient behavior, in which some mass is expelled (due to thermal expansion) into the caprock. After 2000 years, the system is perturbed by withdrawal of mass, simulating natural venting. The pressure boundary at the top of the reservoir is replaced with a no (mass) flow boundary, however, energy is lost to the caprock via conduction. A well is completed in the top grid block of the fracture network, and mass is withdrawn at a rate of 0.4 kg/s, corresponding to a discharge rate of 40 kg/s/km<sup>2</sup>. This discharge rate is similar to estimated natural discharge of many geothermal fields (Pruess, 1985). Fluid is discharged for a period of 20 years, at which time approximately 5% of the initial mass in place has been removed.

The imposed discharge gives rise to rapid boiling in the fractures, which causes cooling at the top of the reservoir. This cooling is partially mitigated by large vertical upflow of vapor, which condenses at the top of the reservoir and releases latent heat. Boiling also occurs in the matrix, though to a lesser extent. At early times large differences in temperatures and pressures exist between fracture and matrix at any given elevation, similar to that noted by Pruess (1985). However, as boiling is induced in the matrix elements, vapor pressure lowering effects cause a reduction in vapor pressure within the matrix, and steam enters the matrix. This influx of steam largely offsets cooling effects of boiling. When

discharge is terminated after 20 years, fracture temperature has fallen by an average of 18°C, and matrix temperature by 5°C. Two phase conditions exist in throughout the fracture system, and in the top 40% of the matrix blocks. The top portion of the fracture network contains a small mobile liquid saturation, characteristic of a vapor-dominated heat pipe. Appreciable liquid ( $S_l > 0.8$ ) exists at depth in the fractures.

After terminating discharge, the reservoir is again isolated and allowed to attain steady state. Heat flux at the base of the reservoir is maintained at 0.5 W/m<sup>2</sup>, and heat loss is allowed through the caprock via conduction. Heat loss does not balance influx for nearly 20,000 years; however, at 10,000 years heat loss to the caprock is 95% of heat influx at the bottom. In attaining steady state, all elements undergo monotonic changes in thermodynamic conditions. Figures 5 - 7 show temperature, pressure, and saturation profiles, respectively, at 10,000 and 30,000 years. These figures clearly show that steady state conditions nearly apply at 10,000 years. Heat loss to the caprock finally balances heat flux applied to the bottom at approximately 20,000 years, and all elements exhibit steady state behavior from that point. Simulations have been run through 100,000 years with virtually no change in the thermodynamic properties in any grid.

Steady state conditions of the reservoir are very interesting. Figures 5 and 6 very clearly show vapor-dominated conditions in the upper 70% of the reservoir, overlying a high temperature reservoir. The pressure gradient in the fractures is slightly in excess of vapor-static, which is sufficient to allow for the downward movement of the small mobile liquid phase. The temperature gradient in Figure 6 also shows the near-isothermal conditions typically found in a vapor-dominated reservoir. Although not shown on these figures, the vapor dominated reservoir came to near steady state about 4,000 years after discharge was terminated. Thermodynamic conditions in the associated matrix blocks are slightly different than adjacent fractures, with temperatures larger by about 4.5° C and pressures less by 700 kPa. The pressure difference causes secondary convection cells to form, with steam moving from fractures to matrix, condensing, and heating the rock.

Below the vapor-dominated reservoir is a transition zone, characterized by relatively large (45%) liquid saturations in the fractures, with a high temperature reservoir below. The transition begins just above the "modified relative permeability zone" in the fractures, and extends downward 200 meters. Mobile liquid in this zone is approximately 5%. This water trickles downward into the high temperature zone, where it is immediately vaporized. No mobile water exists in the HTR in the fracture network, though average liquid saturation in the matrix is about 75%. This lack of liquid in the fractures appears to be directly responsible for the occurrence of high temperatures, as insufficient mass is available for efficient heat pipe behavior. Liquid recharge into this portion of the reservoir is largely due to gravity drainage in the matrix blocks.

While this numerical model is extremely simple relative to real geothermal systems, it shows the possible genesis of a vapor dominated reservoir from a liquid dominated system. One aspect of this vapor-dominated reservoir is the

formation of a steady state, high temperature reservoir below the "typical" reservoir. Use of a zone of reduced mobility in the lower portion of the fractures makes this model similar in some regards to the "permeability barrier model of Drenick (1986). Further studies are planned to examine what effect other causes of reduced mobility at depth have on HTR formation; for example, a decrease in absolute permeability (rather than relative permeability) with depth.

### **Summary and Conclusions**

A numerical study has shown that a high-temperature reservoir can develop as a steady state component of a vapor-dominated reservoir. The reservoir model used here began as a hot water geothermal system. Through simulated natural venting, a perturbation was introduced, during which the reservoir underwent long (> 20,000 years) transient behavior. At termination of the venting, the reservoir moved monotonically toward steady state. Steady state conditions nearly applied at 10,000 years, with heat loss approximately 95% of the heat influx. Steady state prevailed at approximately 20,000 years, and conditions remained constant through a simulated time of 100,000 years. The steady state conditions included a vapor-dominated reservoir overlaying a high temperature reservoir at depth. Matrix liquid saturations are 100% in the "typical" reservoir, and average approximately 75% in the HTR. Saturations in top of the fractures are as typically observed in a vapor-dominated reservoir, with small mobile liquid saturations. No liquid exists in the HTR fractures.

It should be emphasized that several ad hoc assumptions were implemented in this study. In particular, a zone of reduced mobility in the fracture system was used. Insufficient measurements have been made to evaluate the validity of this assumption. Future studies are planned to investigate these and other aspects of this model.

### **Acknowledgements**

I gratefully thank Mark Walters of RREC and Greg Anderson of UNOCAL for many useful conversations on this topic, and Jackie Brower of EG&G for help with manuscript layout. Funding for this work was provided by the U.S. DOE, Assistant Secretary for Conservation & Renewable Energy, Office of Utility Technologies, under DOE Contract No. DE-AC07-76ID01570. Mention of specific products and/or manufacturers in this document implies neither endorsement of preference nor disapproval by the U.S. Government, any of its agencies, of EG&G Idaho, Inc of the use of a specific product for any purpose.

### **References**

Drenick, Andy, "Pressure-Temperature-Spinner Survey in a Well at The Geysers," *Proceedings*, 11th Workshop on Geothermal Reservoir Engineering, Stanford University, Stanford, CA., January 21-23, 1986.

Eastman, G. Y., "The Heat Pipe," *Scientific American*, Vol. 218, 1968, pp 38-46.

Holt, R., and A. Pingol, "Adding Adsorption to a Geothermal Simulator," *Proceedings*, 17th Workshop on Geothermal Reservoir Engineering, Stanford University, Stanford, CA., January 29-31, 1992.

Nghiem, C.P., and H.J. Ramey, "One-Dimensional Steam Flow Under Desorption," *Proceedings*, 16th Workshop on Geothermal Reservoir Engineering, Stanford University, Stanford, CA., January 23-25, 1991.

Pruess, K., Y.W. Tsang, and J.S.Y. Wang, "Modeling of Strongly Heat Driven Flow in Partially Saturated Fractured Porous Media," presented at the IAH 17th International Congress on the Hydrogeology of Rocks of Low Permeability, University of Arizona, 1985.

Pruess, Karsten, "A Quantitative Model of Vapor Dominated Geothermal Reservoirs as Heat Pipes in Fractured Porous Rock," *Transactions*, Geothermal Resource Council, Vol. 9, II, August, 1985.

Pruess, K., R. Celati, C. Calore, and G. Cappetti, "On Fluid and Heat Transfer in Deep Zones of Vapor-Dominated Geothermal Reservoirs," *Proceedings*, 12th Workshop on Geothermal Reservoir Engineering, Stanford University, Stanford, CA., January 20-22, 1987.

Truesdell, A.H., and D.E. White, "Production of Superheated Steam from Vapor-Dominated Geothermal Reservoirs," *Geothermics*, Vol. 2, Nos. 3-4, 1973, pp 154-173,

Truesdell, Alfred H., "The Origin of High-Temperature Zones in Vapor-Dominated Geothermal Systems," *Proceedings*, 16th Workshop on Geothermal Reservoir Engineering, Stanford University, Stanford, CA., January 23-25, 1991.

Vinsome, P.K.W., "TETRAD Users Manual," Dyad Engineering, Calgary, Alberta, Canada, 1991.

Vinsome, P.K.W., and G.M. Shook, "Multi-Purpose Simulation," *J. Petroleum Science and Engineering*, to appear, 1993.

Walters, M.A., J.N. Sternfeld, J.R. Haizlip, A.F. Drenick, and Jim Combs, "A Vapor-Dominated Reservoir Exceeding 600° F at The Geysers Sonoma County, California," *Proceedings*, 13th Workshop on Geothermal Reservoir Engineering, Stanford University, Stanford, CA., January 19-23, 1988.

Warren, J.E., and P.J. Root, "The Behavior of Naturally Fractured Reservoirs", *Society of Petroleum Engin. J.*, Sept. 1963.

White, D.E., L.J.P. Muffler, and A.H. Truesdell, "Vapor-Dominated Hydrothermal Systems Compared with Hot-Water Systems," *Economic Geology*, Vol. 66, 1971, pp 75-97

#### **DISCLAIMER**

This report was prepared as an account of work sponsored by an agency of the United States Government. Neither the United States Government nor any agency thereof, nor any of their employees, makes any warranty, express or implied, or assumes any legal liability or responsibility for the accuracy, completeness, or usefulness of any information, apparatus, product, or process disclosed, or represents that its use would not infringe privately owned rights. Reference herein to any specific commercial product, process, or service by trade name, trademark, manufacturer, or otherwise does not necessarily constitute or imply its endorsement, recommendation, or favoring by the United States Government or any agency thereof. The views and opinions of authors expressed herein do not necessarily state or reflect those of the United States Government or any agency thereof.

**Table 1: Petrophysical Properties and Initial Conditions**

| <b>Petrophysical Properties</b>                | <u>Matrix</u>                 | <u>Fractures</u>            |
|--|-------------------------------|-----------------------------|
| Porosity                                       | 0.04                          | 0.01                        |
| Permeability (md)                              | 0.01                          | 10.                         |
| Relative Permeabilities                        |                               |                             |
| $k_{rl} = k_{rl}^o (S)^{e_l}$                  | $k_{rl}^o = k_{rv}^o = 1$     | $k_{rl}^o = k_{rv}^o = 1$   |
| $k_{rv} = k_{rv}^o (1 - S)^{e_v}$              | $e_l = 4.; e_v = 2.5$         | $e_l = 2.; e_v = 1.5$       |
| $S = \frac{S_l - S_{lr}}{1 - S_{lr} - S_{vr}}$ | $S_{lr} = 0.4; S_{vr} = 0.05$ | $S_{lr} = 0.05; S_{vr} = 0$ |

Rock Heat Capacity = 1. kJ/kg

Rock Density = 2650 kg/m<sup>3</sup>

Rock Thermal Conductivity = 2.1 W/m°C

Matrix Block Size = 100. m

Heat Flux = 0.5 W/m<sup>2</sup>

### **Initial Conditions**

Pressure = Hydrostatic Gradient,  $P_{avg} = 8260$  kPa

Temperature = 240° C

### **Grid Data**

$N_x = 1$

$N_y = 1$

$N_z = 24$

$\Delta x = 100$  m

$\Delta y = 100$  m

$\Delta z = 50$  m

**Figure 1. Matrix Relative Permeability vs. Liquid Saturation.**

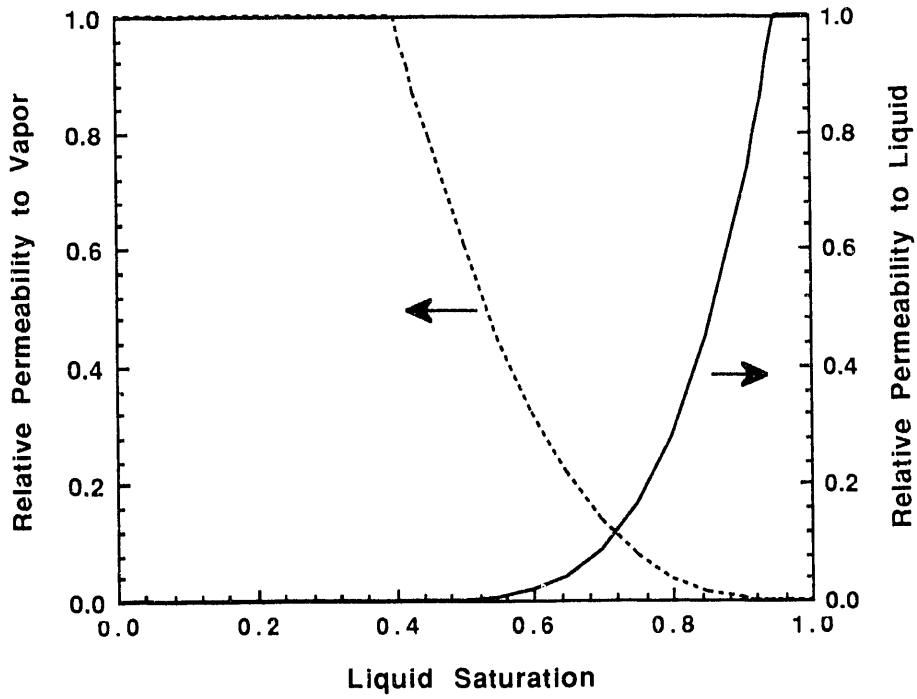


**Figure 2. Fracture Relative Permeability vs. Liquid Saturation.**

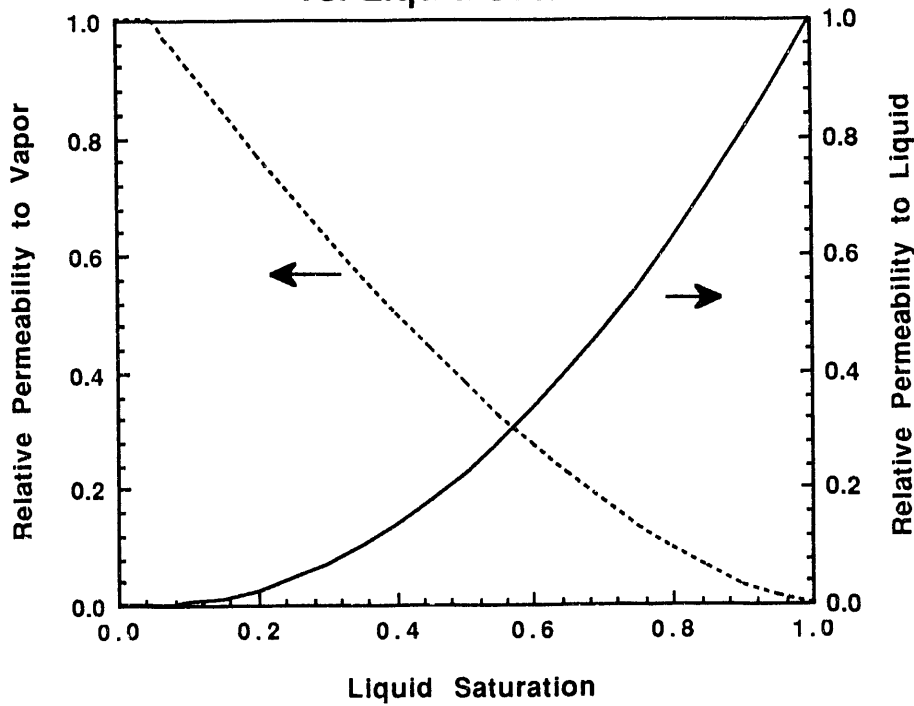


**Figure 3. Capillary Pressure Curves for Matrix and Fracture Grid Blocks.**

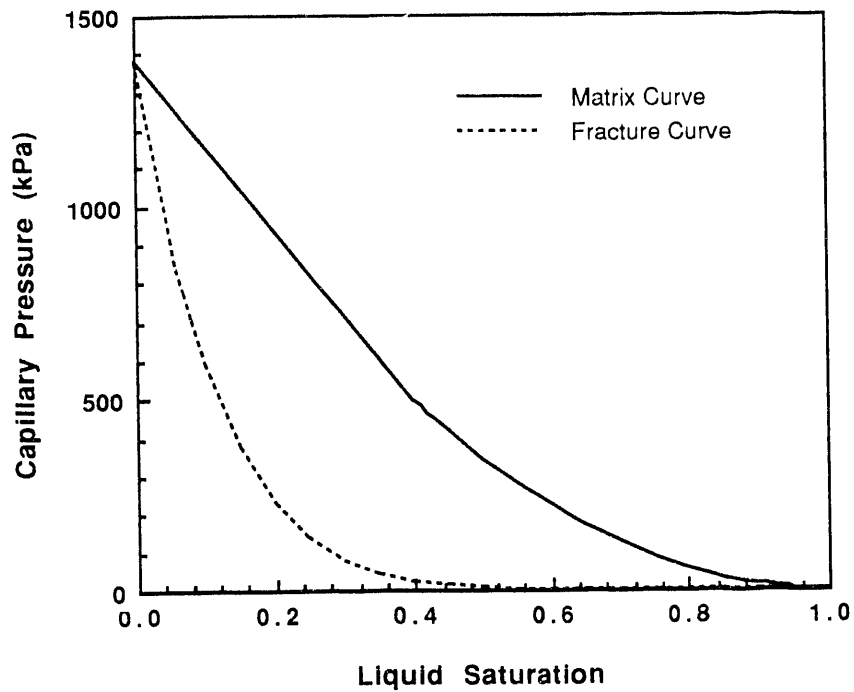


**Figure 4. VPL Effects Used in Model.**

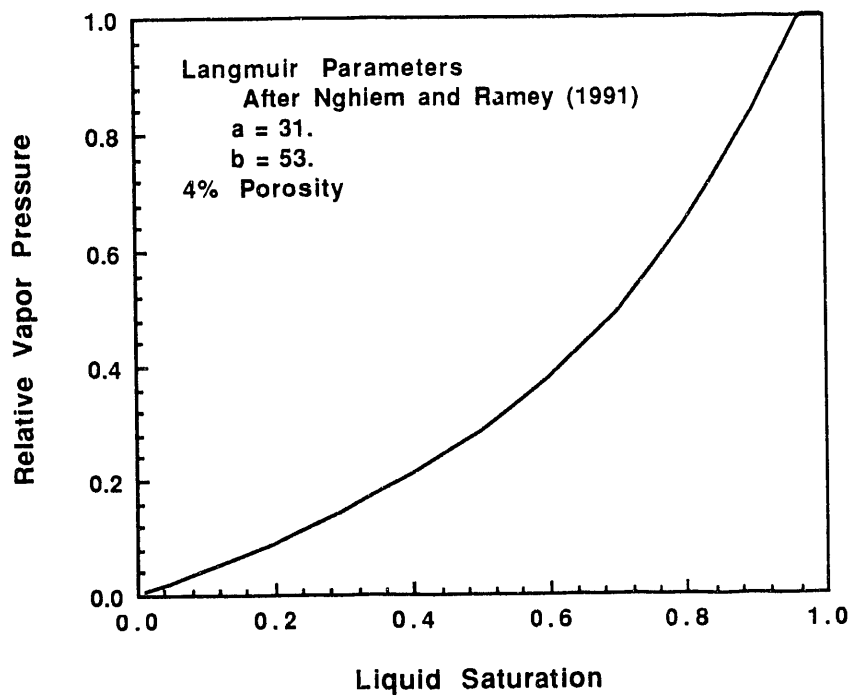


Figure 5. Pressure Profiles for Base Case at 10,000 and 20,000 Years.

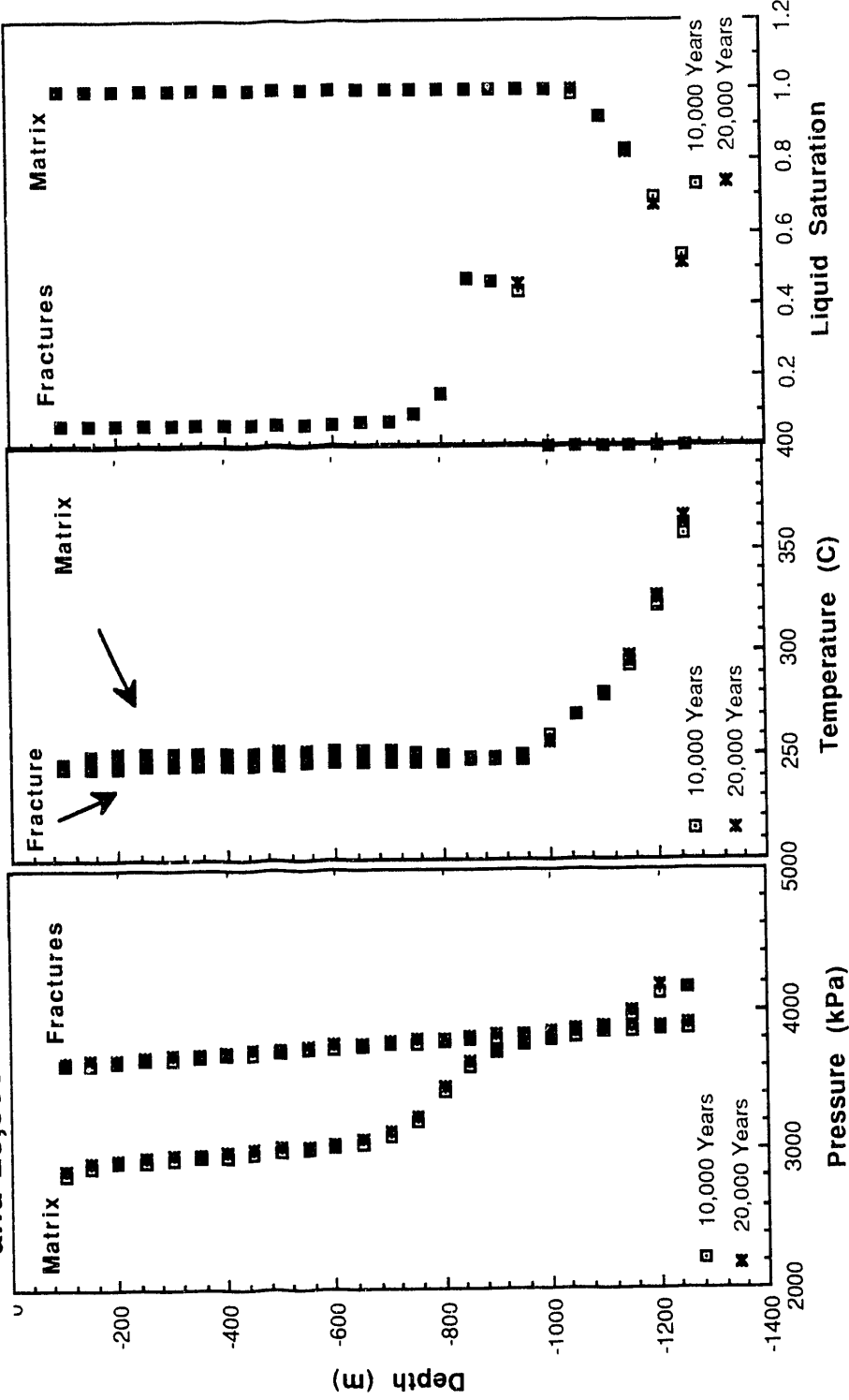


Figure 6. Temperature Profiles for Base Case at 10,000 and 20,000 Years.

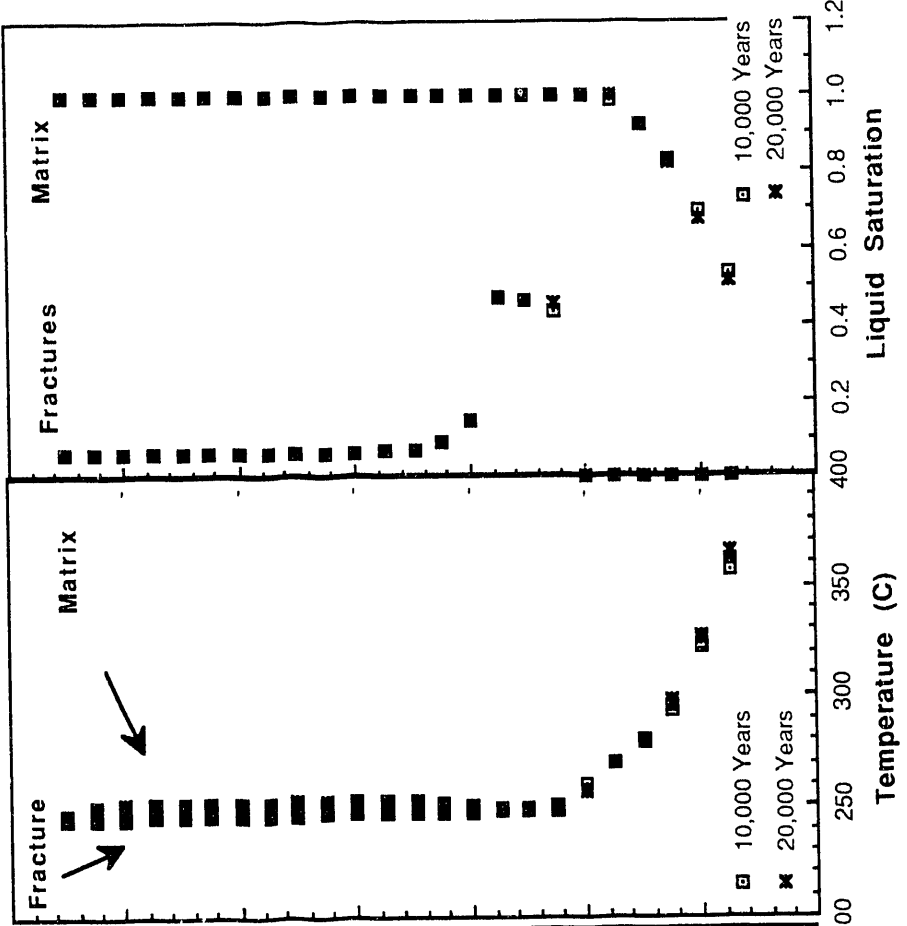
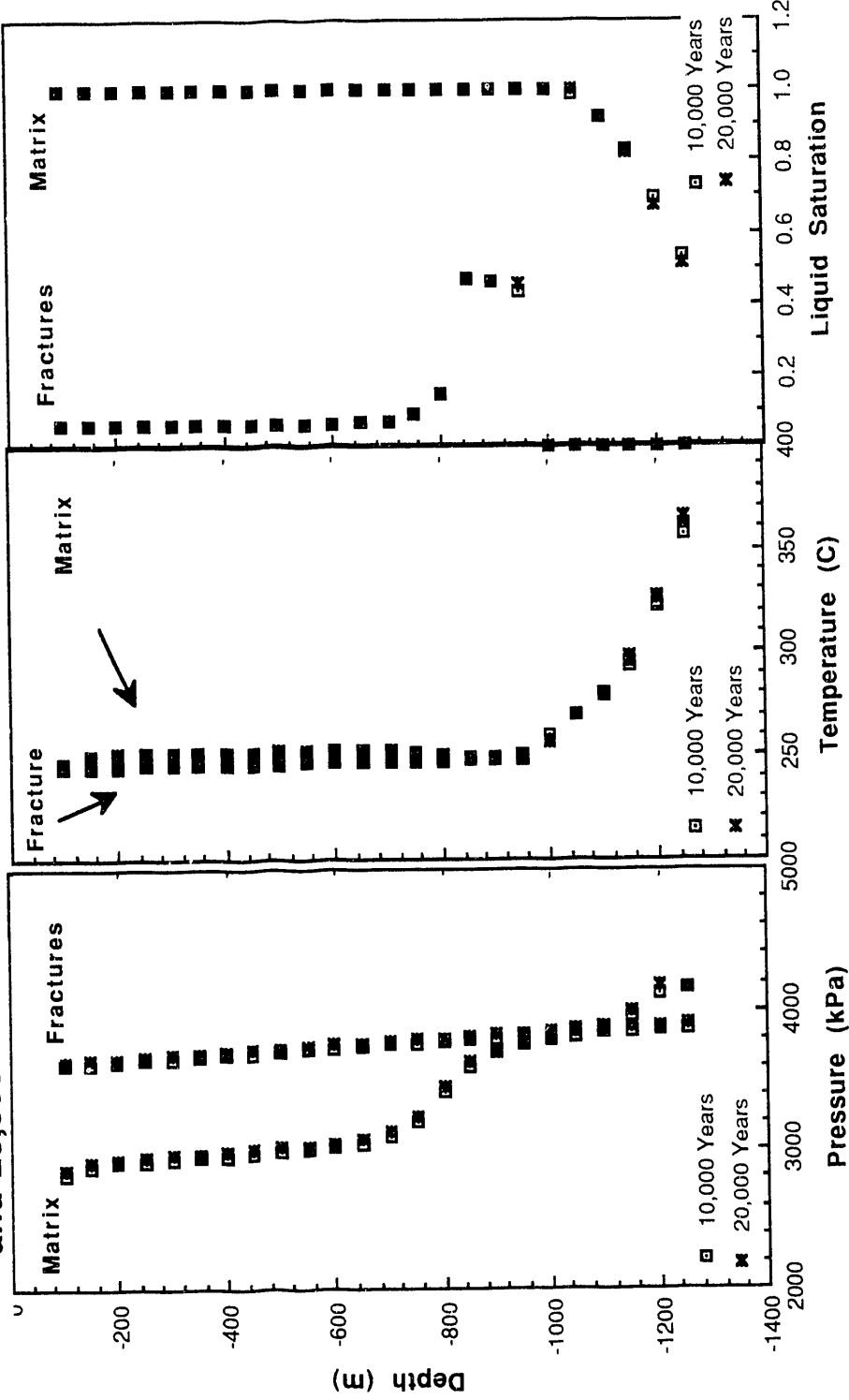


Figure 7. Water Saturation Profiles for Base Case at 10,000 and 20,000 Years.



**DATE**

**FILMED**

8 / 31 / 93

**END**